NASA TECHNICAL NOTE

NASA TN D-3039

EXPERIMENTAL STUDY OF TEMPERATURE DISTRIBUTION IN LAMINAR FLOW OF A HEAT-GENERATING FLUID IN RECTANGULAR CHANNELS

by Mary K. Strite and Robert M. Inman

Lewis Research Center
Cleveland, Ohio

NATIONAL AERONAUTICS AND SPACE ADMINISTRATION • WASHINGTON, D. C. • OCTOBER 1965

NASA TN D-3039

EXPERIMENTAL STUDY OF TEMPERATURE DISTRIBUTION IN LAMINAR FLOW OF A HEAT-GENERATING FLUID IN RECTANGULAR CHANNELS

By Mary K. Strite and Robert M. Inman

Lewis Research Center
Cleveland, Ohio

NATIONAL AERONAUTICS AND SPACE ADMINISTRATION

For sale by the Clearinghouse for Federal Scientific and Technical Information
Springfield, Virginia 22151 – Price $2.00

EXPERIMENTAL STUDY OF TEMPERATURE DISTRIBUTION IN LAMINAR FLOW OF A HEAT-GENERATING FLUID IN RECTANGULAR CHANNELS

by Mary K. Strite and Robert M. Inman

Lewis Research Center

Author

SUMMARY

34246

An experimental investigation was conducted for laminar forced-convection flow of a heat-generating fluid in passages having rectangular cross sections. Wall-temperature measurements were made for fully developed flow in ducts with aspect ratios of 1:1, 4:1, and 8:1, with an approximately uniform heat generation in the fluid stream.

Experimental results are presented for a Reynolds number range from 300 to 1100 and for an internal heat generation rate ranging from 5 000 to 11 500 Btu per hour per cubic foot. These results are compared with theoretical analyses for a parallel-plate channel and for a circular tube.

The results indicated that the wall temperature along the length of the ducts and the longitudinal variation of the difference between the local wall and fluid bulk temperatures can be predicted adequately from the theoretical analyses for the parallel-plate channel, provided the half-length of the short side of the rectangular duct is used as the characteristic dimension. The theoretical analyses for the parallel-plate channel do not correlate the present experimental data along a single line when the hydraulic diameter is used as the characteristic duct dimension. The measurements also revealed that the hydraulic diameter concept, which implies that heat transfer in laminar flow in a noncircular passage can be calculated from, or correlated with, relations for a round tube by use of the hydraulic diameter, is not applicable for laminar heat transfer in rectangular ducts with heat sources in the fluid. The dimensionless thermal entrance length for the rectangular ducts was found to be a constant and independent of aspect ratio.

Author

INTRODUCTION

The last several years have seen an increasing analytical and experimental research effort on the heat-transfer characteristics for fluid flow in ducts with heat generation in

the fluid. The interest in this particular mode of heat transfer has been spurred by the many practical applications in which such flows may occur, for example, in fluid-fueled nuclear reactors, chemical process equipment, magnetohydrodynamic generators, and electromagnetic flowmeters or pumps. In a magnetohydrodynamic generator, for example, the fluid will be heated by the electric current flowing through it and by viscous dissipation. The design and analysis of heat exchange equipment for any of the preceding applications requires a knowledge of the temperature distribution along the duct walls in the presence of the liberation of heat in the flow.

For forced-convection flow in a circular tube, analytical treatment of the heat-transfer characteristics of the heat-generating fluid has been carried out for the fully developed region (ref. 1) and for both the thermal entrance region and the fully developed region (refs. 2 to 5). Experimental studies have been carried out for tube flow for the fully developed region (refs. 6 and 7) and for the thermal entrance region (ref. 8).

Analytical solutions for the heat transfer by forced convection for fluid flow in noncircular ducts with heat generation in the fluid are less prevalent in the literature, presumably because of the complications that an extra space coordinate introduces. Results for a fully developed temperature distribution have appeared for flows in equilateral triangular ducts and elliptical tubes (ref. 9), indented pipes of cardioid section (refs. 10 and 11), and in hexagonal ducts (ref. 11). Up to the present, the heat-transfer characteristics of such passages in the presence of heat liberation in the flow have not been experimentally investigated.

Another duct of noncircular shape that occurs quite frequently in forced-convection heat-transfer applications is the rectangular passage. In order to gain some understanding of the heat-transfer characteristics of such a flow passage and to avoid the added difficulties that would be present in the solution of the problem of a channel with an arbitrary finite aspect ratio, analytical investigations are addressed to the special case of an infinite aspect ratio channel, that is, to the flow between two parallel plates (often referred to as a flat duct). The assumption of an infinite aspect ratio leads to the fluid-flow and heat-transfer situation in which the fluid velocity and temperature depend on only a single cross-section coordinate, for example, the distance from the channel centerline. Such a situation lends itself readily to an analysis of both the thermal entrance region and the fully developed region for a variety of thermal boundary conditions. Results applicable over the entire duct length for the heat-transfer characteristics with laminar flow of a heat-generating fluid in a parallel-plate channel have been given in references 12 to 14. It is generally expected that the solution to the infinite-aspect-ratio channel problem will be applicable to high-aspect-ratio channels and may possibly indicate trends even when the ratio is low. Unfortunately, there are no entrance region or fully developed region calculations in the literature for flows of heat-generating fluids in finite-aspect-ratio channels, so that the designers of heat-transfer equipment for use in

the applications mentioned lack knowledge on whether the results of the previously mentioned investigations are close to reality. An attempt has been made to solve the two-dimensional eigenvalue problem that arises in connection with the analysis of convective heat transfer in the thermal entrance region of a rectangular duct (ref. 15), but the method is presently inadequate for the designer, and no additional work has apparently been done along these lines.

It might be expected that the finite aspect ratio of a practical channel will conceivably give rise to a surface temperature that varies around the periphery of the duct in some part, or in all parts, of the thermal entrance region, or to a wall-to-bulk temperature difference that is greater in some part of the entrance-region than it is in the fully developed region. Such conceivable effects, or other at-present unknown temperature variations, would not be predicted by the parallel-plate channel analysis, since in this configuration peripheral temperature variations are absent, the fully developed velocity profile is one-dimensional, and the wall-to-bulk temperature difference in the entrance region is always less than the fully developed difference. The designer is necessarily interested in any such foregoing possibilities and, moreover, is interested in (1) determining the location where the wall temperature of a rectangular passage containing a flowing, heat-generating fluid assumes its highest value, (2) obtaining knowledge of the heat-transfer conditions in the corner regions of such ducts, (3) determining a duct dimension that provides correlation of heat-transfer data for finite-aspect-ratio ducts with parallel-plate channel results, and (4) determining if the heat-transfer performance of a noncircular duct can be obtained with good accuracy from relations for a circular duct through the use of the hydraulic diameter as the characteristic dimension of the noncircular passage.

There are no experimental measurements for the forced-convection heat transfer in the flow of a heat-generating fluid in rectangular passages, so that an understanding of convective heat transfer under these conditions is limited to the results of parallel-plate channel analyses. In view of this limitation, it appeared worthwhile to investigate the heat-transfer characteristics of rectangular ducts of different aspect ratios and containing heat-generating fluids with the particular aim of determining whether the wall temperature variation (longitudinal as well as peripheral) and longitudinal variation of wall-to bulk-temperature difference are affected by changes in the duct aspect ratio. It is to be expected that the parallel-plate channel represents the limiting situation for the rectangular duct as the aspect ratio becomes large. The parallel-plate channel analyses have considered laminar flow, and hence it seemed natural to limit the experimental investigation to laminar flow in the rectangular passages.

This report presents and discusses the experimental studies that have been made on the velocity distribution, longitudinal and peripheral wall temperature variation, and longitudinal variation of the difference between the local wall temperature and the fluid

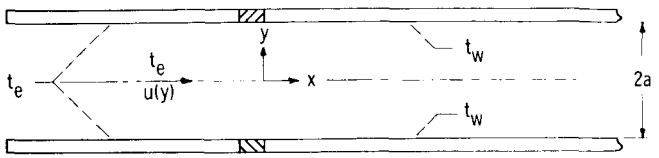

Figure 1. - Physical model and coordinate system for parallel-plate channel.

bulk temperature for laminar incompressible flow of a heat-generating fluid in insulated rectangular ducts with aspect ratios of 8:1, 4:1, and 1:1. The heat generation in each duct was essentially longitudinally and transversely uniform and the velocity profile fully developed. The experimental results for the temperature distributions obtained for the three rectangular ducts are compared with the analytical results obtained for the parallel-plate channel. All ducts were of the same construction and materials, differing only in cross section and overall length.

The solution to the problem of laminar flow of a fluid in an insulated parallel-plate channel with uniform internal heat generation is reviewed here to make the study more complete.

LAMINAR FULLY DEVELOPED FLOW BETWEEN INSULATED PARALLEL PLATES WITH UNIFORM INTERNAL HEAT GENERATION

The problem of Poiseuille flow between parallel plates with uniform internal heat generation in the fluid and zero wall heat transfer has been considered in references 12 to 14 and is only briefly reviewed.

The geometry under consideration is illustrated in figure 1. The fluid flows from left to right. The part of the channel to the left of $x = 0$ is an unheated hydrodynamic starting length used to obtain fully developed flow at the entrance to that portion of the duct where an internal heat generation takes place in the fluid ($x > 0$). The height of the channel (i.e., the distance between the plates) is 2a, and y is the transverse coordinate measuring distances from the channel centerline.

The energy equation for laminar flow in a parallel-plate channel and with uniform internal heat generation in the fluid can be written as

$$\rho c_p u \frac{\partial t}{\partial x} = \kappa \frac{\partial^2 t}{\partial y^2} + Q \tag{1}$$

(All symbols are defined in appendix A.) Fluid properties have been assumed constant, and viscous dissipation and longitudinal conduction have been considered negligible compared with transverse conduction. The heat source term is assumed constant.

When the boundary conditions $\partial t/\partial y = 0$ at $y = a$ and $-a$ (zero wall heat transfer) and $t = t_e$ at $x = 0$ (specified uniform entrance temperature), in addition to the plane

Poiseuille velocity distribution

$$u = \frac{3}{2}\bar{u}\left(1 - \frac{y^2}{a^2}\right)$$

are used, the solution for the temperature which applies in both the thermal entrance and fully developed regions is given by

$$\frac{t - t_e}{(Qa^2/\kappa)} = 4\frac{x/2a}{RePr} + \frac{1}{4}\left[\left(\frac{y}{a}\right)^2 - \frac{1}{2}\left(\frac{y}{a}\right)^4 - \frac{11}{70}\right] + \sum_{n=1}^{\infty} A_n Y_n \exp\left(-\frac{4\lambda_n^2}{RePr}\frac{x}{2a}\right) \tag{2}$$

where λ_n^2 and Y_n are, respectively, the eigenvalues and eigenfunctions of the Sturm-Liouville problem

$$\frac{d^2Y_n}{d(y/a)^2} + \frac{3}{2}\lambda_n^2\left[1 - \left(\frac{y}{a}\right)^2\right]Y_n = 0 \tag{3a}$$

$$\frac{dY_n}{d(y/a)} = 0 \quad \text{at} \quad y = 0 \quad \text{and} \quad y = a \tag{3b}$$

The first several eigenvalues λ_n^2, eigenfunctions $Y_n(1)$, and coefficients A_n have been computed and listed in references 12 to 14.

The wall temperature variation corresponding to the uniform heat generation is obtained by setting $y = a$ in equation (2), which yields

$$\frac{t_w - t_e}{Qa^2/\kappa} = 4\frac{x/2a}{RePr} + \frac{3}{35} + \sum_{n=1}^{\infty} A_n Y_n(1)\exp\left[-\frac{4\lambda_n^2}{RePr}\left(\frac{x}{2a}\right)\right] \tag{4}$$

The fluid bulk temperature, for a uniform heat source, is obtained from the definition

$$t_b(x) - t_e = \frac{Q}{\rho\bar{u}c_p}x = 4\left(\frac{Qa^2}{\kappa}\right)\left(\frac{x/2a}{RePr}\right) \tag{5}$$

Then the difference between the wall and bulk temperatures at any longitudinal location

x is given by

$$\frac{t_w - t_b}{Qa^2/\kappa} = \frac{3}{35} + \sum_{n=1}^{\infty} A_n Y_n(1) \exp\left[-\frac{4\lambda_n^2}{RePr}\left(\frac{x}{2a}\right)\right] \tag{6}$$

Equations (4) to (6) will serve as bases of comparison for the experimental data obtained from the three rectangular ducts.

EXPERIMENTAL APPARATUS

Three rectangular ducts of aspect ratios 8:1, 4:1, and 1:1 were used in the present investigation. A schematic diagram of the experimental apparatus applicable to the three ducts is shown in figure 2. Table I gives the dimensions of each duct.

An aqueous electrolyte solution (dilute sodium chloride) was pumped from the reservoir through an unheated entrance section and into the insulated test section, where the fluid was resistance heated. Internal heat generation was achieved by passing an electric current through the fluid. After leaving the heating section, the fluid flowed through an insulated mixing chamber where the exit bulk temperature was measured, through a heat exchanger, and finally returned to the reservoir for recirculation. Between the entrance and heating sections and between the heating and mixing sections there was situated an electrode of hollow rectangular profile whose inner dimensions matched those of the sections. The electrode and lucite sections were separated from one another by neoprene or rubber gaskets 0.125 inch thick.

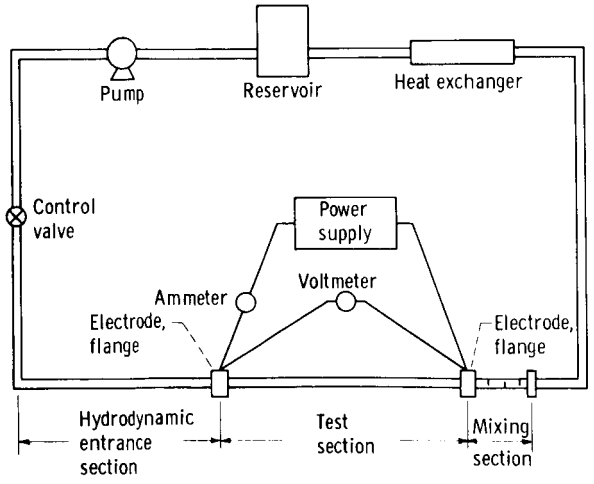

Figure 2. - Schematic diagram of test apparatus.

TABLE I. - DUCT DIMENSIONS

[All dimensions in inches.]

Aspect ratio (nominal)	Width 2b (±0.010)	Height 2a (±0.010)	Length of unheated section	Length of test section
8:1	8.000	1.000	68.0	96
4:1	4.000	1.000	69.5	84
1:1	1.000	1.000	60.5	84

An unheated starting length was used to obtain hydrodynamically fully developed flow at the entrance to the heating section. The duct walls were constructed from 0.500-inch-thick lucite plates. The top wall was provided with thermocouple wells and two small openings in the wall for the insertion of a hypodermic needle into the fluid stream. This section was covered with 1-inch fiber glass blanket insulation. The hydrodynamic entrance length, which is defined as where 99 percent of the fully developed centerline velocity is attained, was determined for each duct from the analytical results given in reference 16. In the ducts of aspect ratios of 4:1 and 1:1, a few test conditions were encountered where later calculations indicated that the centerline velocity was (theoretically) 90 to 93 percent of the fully established velocity. For the duct with an aspect ratio of 8:1 the entrance length was longer than necessary for all runs.

The heating section, or test section, walls were likewise constructed from 0.500-inch-thick lucite plates. The top wall was provided with thermocouple wells distributed transversely at specific longitudinal positions. The length of the test section for each aspect ratio was selected after consideration of (1) power supply limitation (1.33 kW), (2) maximum desired fluid bulk-temperature rise (approximately 6.0° F), and (3) minimum desired Reynolds number for the flow (approximately 300). The length chosen for each investigation represented a compromise between these three restrictions. This section was likewise covered with 1-inch fiber glass blanket insulation.

The mixing section walls were constructed from 0.500-inch-thick lucite plates and the chamber was approximately 8 inches in length. This section contained three lucite baffles, cemented into the chamber and alined perpendicular to the flow. These baffles contained several holes of various diameters, and the holes were misalined from baffle to baffle to further induce mixing of the fluid. Three thermocouple wells, distributed transversely, were located downstream of the baffles for the measurement of the exit bulk temperature. This section was insulated with a 1-inch fiber glass blanket insulation. Following the mixing section was a duct portion in which the cross section changed from the rectangular shape to a circular one.

A counterflow heat exchanger was used to cool the circulating fluid after it was heated in the test section. This exchanger consisted of two concentric copper tubes that were 3 feet in length and had inside diameters of 0.5 and 1.0 inch, respectively. The inner surface of the smaller tube was coated with a corrosion-resistant paint.

The reservoir consisted of a 50-gallon-capacity stainless-steel tank. A 1/8-horsepower centrifugal pump was used to circulate the fluid and was fed by the reservoir. A manually operated control valve, placed upstream of the entrance transition duct, was used to regulate the flow. The various lucite sections were bolted to one another through special flanges. The flanges at either end of the test section contained cutout regions into which were inserted the electrodes. The electrodes were therefore completely encased within a lucite covering.

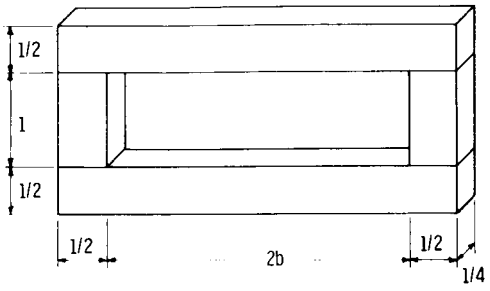

Figure 3. - Typical electrode shape and dimensions. Material, graphite. (All dimensions are in inches.)

Electrical power, used for heating the fluid, was supplied by a 400-cycle-per-second single-phase power supply, which had a maximum output of 70 volts and 19 amperes. A 4:1 transformer was used to boost the voltage being supplied to the test section. Electric power was applied to the fluid by means of the two graphite electrodes. The electrode assemblage consisted of rectangular sticks of graphite cemented together to form an electrode of a hollow rectangular shape. Electrode shape and dimensions are illustrated in figure 3. The dimension 2b was 8.0, 4.0, and 1.0 inch for the ducts with aspect ratios of 8:1, 4:1, and 1:1, respectively. Each electrode was made thin (1/4 in. thickness) to minimize end effects and was wrapped with a thin strip of copper to which was attached a power lead.

A 400-cycle alternating current was selected for these investigations to prevent electrolysis of the aqueous electrolyte solution. For the maximum impressed voltage and current flow used in the experimental program (260 V and 3.60 A), there was no visible evidence of electrolysis.

The voltage measurements were made with a 50 to 400 cycle per second voltmeter with an accuracy of 1/2 percent of full scale. The current flow was measured with 400 cycle per second ammeter, which had a calibrated accuracy of 1/2 percent full scale. For the lower currents that were encountered in the investigation of the duct of aspect ratio 1:1, an ammeter with a range of 0 to 1.0 ampere was calibrated and used to determine the current flow.

The internal heat generation was achieved, as mentioned earlier, by directing a 400-cycle alternating current through the aqueous electrolyte solution. Since an electric current was passing through the fluid, the return loop of the system constituted another branch for current flow; hence, the electrical resistance of that branch had to be made large relative to that of the test section in order to prevent or minimize current leakage out of the heating section. Initially this was accomplished (1) by lengthening the return loop relative to the length of the test section through the addition of long lengths of rubber hose and (2) by reducing the cross-sectional area of the return loop relative to that of the test section. It was estimated that the resistance of the return loop was about 96 times that of the test section for the duct of aspect ratio 8:1, and about 48 times that of the test section for the duct of aspect ratio 4:1. For the investigation of the duct of aspect ratio 1:1, the existing return loop setup offered a resistance ratio of only about 10:1; it was, therefore, necessary to increase the resistance of the return loop still more. This was accomplished by the insertion of a splash plate in the reservoir, which served to break up the returning fluid into droplets, thereby stopping the electric circuit flow in the re-

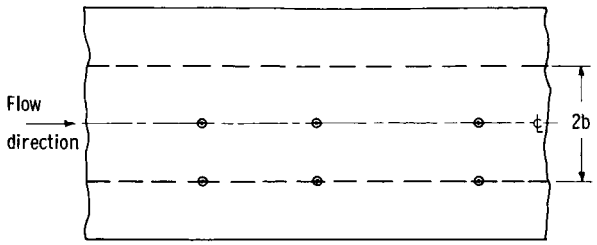

(a) Schematic of top view of channel showing typical thermocouple locations.

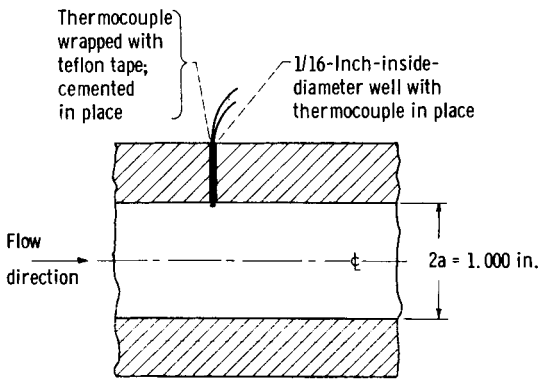

(b) Installation detail.

Figure 4. - Typical thermocouple.

turn loop. All metallic instruments and equipment were isolated from ground to prevent current leakage.

Thermocouples used in this investigation were taken from calibrated rolls of 30-gage iron-constantan thermocouple wire. The thermocouples were cemented in 1/16-inch-diameter walls, which extended completely through the lucite top plate so that the thermocouples were in intimate contact with the surface of the fluid. Initially thermocouples were located at the midplane of the top wall and in the corner at the intersection of the top wall and a side wall at several longitudinal positions. Details of a typical installation can be seen in figure 4. As will be described on page 23, further measurements were made of the transverse temperature distribution by the addition of more thermocouples across the span of the top plate at the various longitudinal positions. Because of the large voltage impressed on the system, as well as the current flow past the thermocouples, it was necessary to isolate each thermocouple from the others when a reading was being taken. This isolation was accomplished by using alternate positions on nonshorting tap switches. The thermocouple outputs were read with a temperature potentiometer, reading directly in degrees Fahrenheit, with a precision of $\pm 0.1^{\circ}$ F. The effect of the additional electromotive force impressed on the thermocouples on the experimental results is unknown; but this effect is believed to be minimized, because the data are presented in the form of temperature differences with this effect included in each thermocouple output to about the same degree of contribution. Fluid flow rates were obtained by measurement of the quantity of fluid collected in a measured time. Table II (p. 10) summarizes the main experimental data.

To substantiate the assumption that fully developed flow conditions existed at the entrance to the heating section, the velocity field of the flow through the duct was measured in a plane located 64 inches from the entrance of the duct of aspect ratio 8:1, 67 inches from the entrance of the duct of aspect ratio 4:1, and in planes located 55.5 and 57.5 inches from the entrance of the duct of aspect ratio 1:1. The velocity distribution was determined by a dye-displacement technique. A traversing mechanism was located at the planes indicated. The mechanism consisted in part of a 20-gage stainless-steel hypoder-

TABLE II. - SUMMARY OF MAIN EXPERIMENTAL DATA

Run	Inlet bulk temperature, ^{o}F	Outlet bulk temperature, ^{o}F	Fluid flow, lb/min	Voltage across test section, V	Current through test section, A
Aspect ratio, 8:1					
8-1	80.9	84.6	10.55	235	3.03
8-2	81.0	86.4	7.19	220	3.09
8-3	78.5	82.3	10.70	235	3.20
8-4	79.0	84.0	7.20	215	3.10
8-6	81.5	85.8	9.53	220	3.32
8-9	80.5	85.0	12.00	260	3.60
8-10	80.6	85.5	10.17	250	3.51
8-11	81.2	86.5	8.56	240	3.42
8-12	81.3	86.8	7.50	230	3.23
Aspect ratio, 4:1					
4-1	80.5	83.5	8.80	236	1.91
4-2	80.5	84.0	7.75	235	2.01
4-3	81.5	86.0	5.94	230	1.99
4-4	86.3	90.3	8.00	238	2.30
4-6	86.9	92.9	4.90	220	2.21
4-7	79.4	82.2	10.00	260	1.89
4-8	80.2	84.9	5.55	248	1.80
Aspect ratio, 1:1					
1-1	88.2	93.3	1.70	260	0.56
1-3	88.3	93.2	1.90	270	.58
1-4	89.2	95.1	1.45	271	.57
1-5	83.2	86.4	2.90	260	.62
1-6	83.7	88.1	2.07	260	.62
1-7	86.0	91.6	1.50	250	.61

mic needle, inserted perpendicular to the flow through a provision made in the duct top wall, with a portion of the needle bent to face downstream. A hypodermic syringe was attached to the needle. The syringe was filled with a dye which was injected in droplets into the fluid through the needle. The time required for a droplet to move a prescribed distance along the flow direction was noted. The location of the needle tip within the duct was accurately determined by the use of a micrometer head, with divisions of 0.001 inch, rigidly secured to the syringe and needle. The entire mechanism was clamped to the duct at the desired location. Details of this mechanism can be seen in figure 5, which shows the device in place for measurements in the duct of aspect ratio 8:1. It was felt that the needle diameter was small enough with respect to the duct dimensions to produce a negligible interference with the velocity field. The velocity measurements were com-

pared with approximate, theoretical, fully developed profiles for laminar incompressible flow in rectangular ducts that are available in the literature (refs. 16 to 18).

RESULTS OF EXPERIMENTAL PROGRAM

Velocity Profiles

The first investigations for each duct were concerned with whether the flow was fully developed. As described, the velocity field of the flow through the duct was measured in a plane located a specific distance from the entrance of the duct. Figure 6 shows the coordinate system for a rectangular duct that will be considered in describing locations in a plane. The longitudinal coordinate x has its origin at the entrance of the heating section.

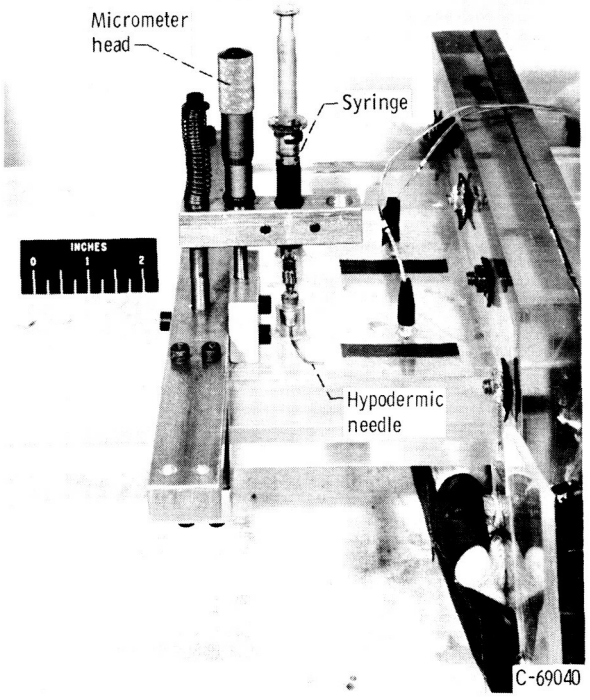

Figure 5. - Velocity probe for 8:1 aspect ratio duct.

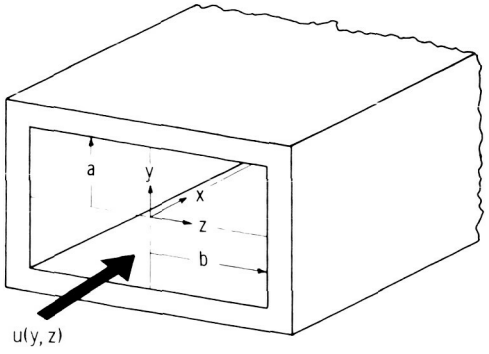

Figure 6. - Coordinate system for rectangular duct. Dimension a, 0.500 inch.

The test fluid (water) was circulated through the system, which was initially inclined approximately 10^{o} from the horizontal in order to remove air bubbles entrained in the fluid. When this removal was accomplished, the system was returned to the horizontal position and the desired flow rate set through the use of the control valve and fluid weight measurement. Velocity surveys were made in one direction perpendicular to the flow and at different Reynolds numbers. Velocity profiles were measured along the vertical planes at $Z = 0$ and 0.75 for the ducts of aspect ratios 8:1 and 1:1, and only along the plane $Z = 0$ for the duct of aspect ratio 4:1. The Reynolds numbers at which the various profiles were taken were 325 and 387, 480 and 536, and 328 and 470 for the 1:1, 4:1, and 8:1 ducts, respectively.

Mention should be made at this point that velocity measurements were made in the absence of power dissipation in the test section;

however, calculations have shown that for the type of fluid and power dissipation used in this investigation, the electrohydrodynamic effect on the velocity distribution is negligible.

An approximation for the velocity distribution in a flat rectangular duct can be taken directly from the solution of the corresponding torsion problem in the theory of elasticity (ref. 17, p. 285, and ref. 18):

$$\frac{u(Y, Z)}{\bar{u}} = \frac{3}{2}(1 - Y^2)\frac{1 - e^{-\gamma\sqrt{\frac{5}{2}}(1-Z)}}{1 - \frac{0.632}{\gamma}} \tag{7}$$

where $Y = y/a$, $Z = z/b$, and $\gamma = b/a$. It is noted that this form is not symmetric in Z and as written only applies when Z is positive. Equation (7) becomes increasingly more accurate as $\gamma \to \infty$ (parallel-plate channel) and increasingly less accurate as $\gamma \to 1$ (square duct). For example, if $\gamma \to \infty$ in equation (7),

$$\frac{u(Y)}{\bar{u}} = \frac{3}{2}(1 - Y^2) \tag{8a}$$

which is the plane Poiseuille velocity profile for flow between parallel plates. On the other hand, if $\gamma = 1$ and $Y = Z = 0$ in equation (7), there is obtained for the ratio of centerline-to-mean velocity for a square duct

$$\frac{u(0, 0)}{\bar{u}} = 3.230 \tag{8b}$$

whereas reference 16 lists for a square duct the result $u(0, 0)/\bar{u} = 2.097$. A more accurate approximation to the laminar velocity distribution in a square duct is also available from the corresponding solution of the torsion problem (ref. 17, p. 283, and ref. 18):

$$\frac{u(Y, Z)}{\bar{u}} = \frac{1}{0.2808}(1 - Z^2)(1 - Y^2)\left[0.5844 + 0.1185(Y^2 + Z^2)\right] \tag{9}$$

In particular, it is noted that setting $Y = Z = 0$ in equation (9) yields the result $u(0, 0)/\bar{u} = 2.070$, which is in good agreement with the result given in reference 16.

Equation (7) was used as the analytical representation of the velocity profile for the 8:1 and 4:1 ducts, while equation (9) was used for the square duct profile.

Figures 7 show a comparison between experimental and theoretical velocity profiles for the three aspect ratios. In these figures, the experimental points are compared

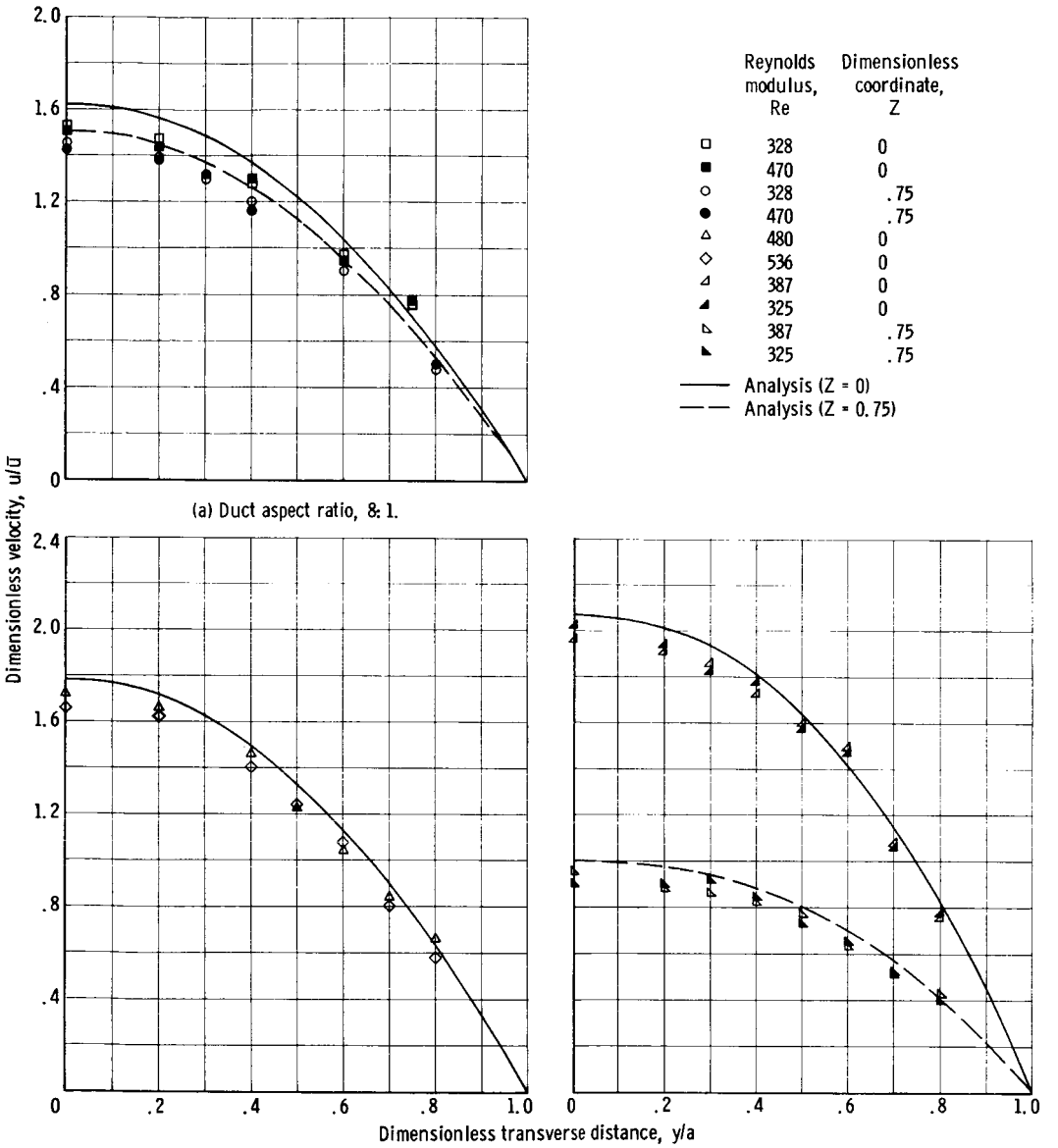

Figure 7. - Comparison of theoretical analysis and experimental results of velocity distribution for laminar flow in a rectangular passage.

with a profile calculated from the appropriate analytical representation. These measurements indicate good agreement between the theoretical and experimental points, within the limits of experimental accuracy, and suggest that the hydrodynamic entry lengths are sufficient to obtain fully developed flow conditions at the entrance to the heating section. Attention is now turned to the investigations of wall temperature distributions.

Wall Temperature Variations

A 3 to 5 percent-by-weight aqueous electrolyte solution was circulated through the system at a prescribed flow rate, which was set through the use of the control valve and fluid weight measurements. Water drawn from the central supply mains was supplied to the heat exchanger to serve as a coolant. Simultaneously, electrical power to be used for heating the electrolytic solution was turned on. The voltage and coolant flow rate were adjusted for a given fluid flow rate until the entrance and exit bulk temperatures of the fluid were invariant with time (variation less than 0.2° F/30.0 min), and the exit bulk temperature did not exceed the entrance bulk temperature by more than 6° F. When these conditions were satisfied, incoming and outgoing fluid bulk temperatures, wall temperatures, fluid flow rate, current flow through the fluid, and voltage drop across the test duct length were measured and recorded.

As previously mentioned, the maximum bulk temperature difference in the experiments was approximately 6.0° F. It was felt that with this reasonably small difference, the variation of physical properties of the fluid (in particular the viscosity) with temperature would be small enough so that the assumption of constant property values would be fulfilled to a reasonable degree. The properties were evaluated at the length-mean bulk temperature.

An additional reason for maintaining a reasonably small bulk-temperature change was to minimize the effects of free convection that frequently arise when low flow velocities, necessary for laminar flow, are employed. The fluid bulk temperature gradient was therefore small and never exceeded 0.9° F per linear foot. The possible effects of free convection on the experimental data will be examined and discussed in more detail later in the section Effect of Free Convection. It suffices to state at this point that the upper limit of the bulk-temperature-gradient range of the experimental data lies below, and the lower limit of the Reynolds number range lies above, the limit at which free convection effects are believed to be noticeable.

The wall thermocouples were located at $Z = 0$ and 1 at the top plate ($Y = 1$) at specific longitudinal positions. It was expected that the temperature at these two locations would be of principle interest to the design engineer.

Heat-transfer measurements were made in each of the three ducts for a moderate range of fluid flow rates. The Reynolds number range of the runs was approximately 300 to 550, 475 to 900, and 575 to 1100 for the 8:1, 4:1, and 1:1 ducts, respectively. There was also a 5 to 15 percent variation in the Prandtl number for the three aspect ratio ducts.

In order to make meaningful comparisons of the experimental data with the results of the theoretical analysis for the parallel-plate channel discussed earlier, it is necessary to determine the heat source distribution throughout the test section.

The maximum bulk temperature difference for the runs was approximately 6° F. With this small difference the electrical resistivity of the fluid is essentially constant, and it can be concluded that the heat source is longitudinally uniform, except in the immediate neighborhood of the electrodes (these nonuniform regions, however, constitute only about 1 percent of the overall test section length and can be neglected).

Transversely variable internal heat generation can arise from electrical skin effect and/or electrochemical side effects. The skin effect phenomenon, which is associated with high-frequency current flow in a conductor, is discussed in reference 19, for example. Calculations based on equations given in reference 19 for the current distribution in a flat or plane conductor show that, for the electrical properties of the conductor and the frequency of current flow chosen for this experiment, the skin effect is negligible; that is, the current flow is not concentrated in a layer or skin near the surface, but is instead distributed uniformly over the cross section.

The more important electrochemical side effects that might be present at the fluid-solid interface are believed to be the phenomena of electrolysis and polarization (refs. 20 and 21). The use of graphite electrodes and a rapidly alternating current satisfactorily minimize or even eliminate these effects (refs. 20 and 21).

On the basis of the foregoing discussions, it is inferred that the heat generation should be essentially longitudinally and transversely uniform. Inasmuch as the heat generation is considered uniform, the fluid bulk temperature rise is given by equation (5):

$$t_b(x) - t_e = \frac{Q}{\rho \bar{u} c_p} x \tag{5}$$

If $x = L$ in equation (5), the result can be written alternatively as

$$(\rho \bar{u} A_c) c_p \left[t_b(L) - t_e \right] = Q A_c L$$

or

$$w c_p \left[t_b(L) - t_e \right] = q_e \tag{10}$$

where q_e is calculated from measurements of the electrical heat input. Equation (10) indicates a heat balance between the electrical heat input and the enthalpy rise of the heat-generating fluid flowing through the duct.

The temperature of the fluid at the entrance to the heating section was 68° to 90° F, and at the outlet about 3° to 6° F above the inlet temperature.

Figure 8 (p. 16) shows the enthalpy rise of the flowing fluid plotted against the elec-

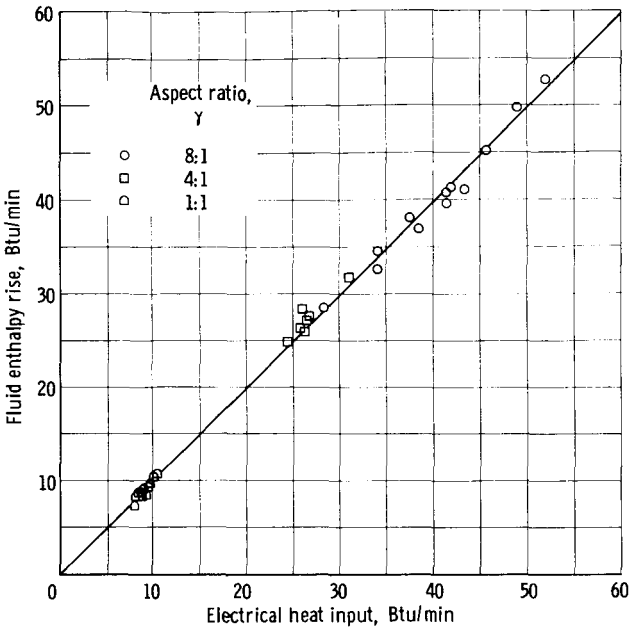

Figure 8. - Comparison of electrical heat input and fluid enthalpy rise for laminar flow in an insulated rectangular passage.

trical heat input. The data points on the figure are the experimental results for the three aspect ratio ducts, and the curve is the result given by equation (10). The physical properties of the fluid were obtained from references 22 and 23 and were evaluated, as mentioned previously, at the length-mean bulk temperature. The experimental points agree satisfactorily with the theoretical solution, which is some evidence of the validity of the assumption of essentially uniform heat generation and of the experimental method used. In general, the heat balances are accurate to about 3 to 6 percent.

The results that are of practical interest are the wall temperature variations in each of the three ducts corresponding to the uniform internal heat source. The experimental data collected for each of the three ducts are shown in figures 9 and 10 in comparison with a curve calculated from the theoretical relation equation (4) and using the numerical data listed in references 12 to 14. The Reynolds and Prandtl numbers that characterize each temperature distribution are based on length-mean bulk properties.

The longitudinal distribution of the temperature difference $t_w - t_e$ measured at the centerline of the top wall (Y = 1, Z = 0) and in a corner of the duct (Y = 1, Z = 1) are presented in dimensionless form in figures 9 and 10, respectively, for the 8:1, 4:1, and 1:1 ducts. The abscissa in each of the figures is the reciprocal of the Graetz number. It is to be noted that the characteristic dimension in both the heat source parameter Qa^2/κ and in the Reynolds number Re is the duct half height a.

It is observed from figure 9(a) that the measured dimensionless wall- to entrance-temperature difference at the centerline falls just slightly above the theoretical for the 8:1 duct; however, apart from some scatter (±10 percent), the data exhibit reasonable agreement with the calculated result for a parallel-plate channel. Figures 9(b) and (c) represent the dimensionless centerline temperature distributions in the 4:1 and 1:1 ducts, respectively; it can be observed that the experimental data and the theoretical curve for the parallel-plate channel are in good agreement (deviation less than 10 percent). The experimental data of figures 9(b) and (c) do not extend beyond a value of 0.03 for the reciprocal of the Graetz number because the test sections are too short.

In figure 10(a) data is shown for the dimensionless wall- to entrance-temperature

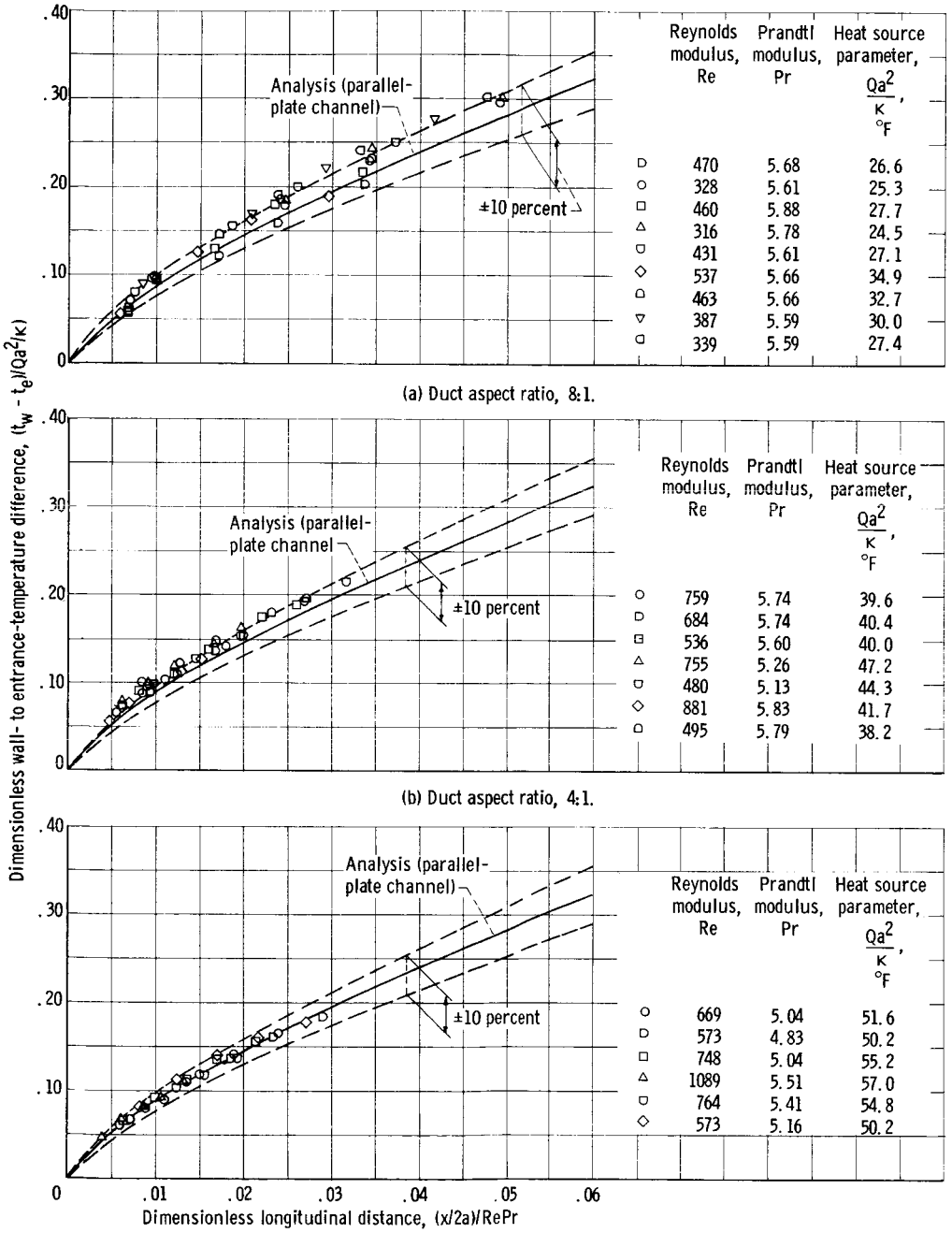

Figure 9. - Longitudinal variation of wall- to entrance-temperature difference measured at centerline of top wall.

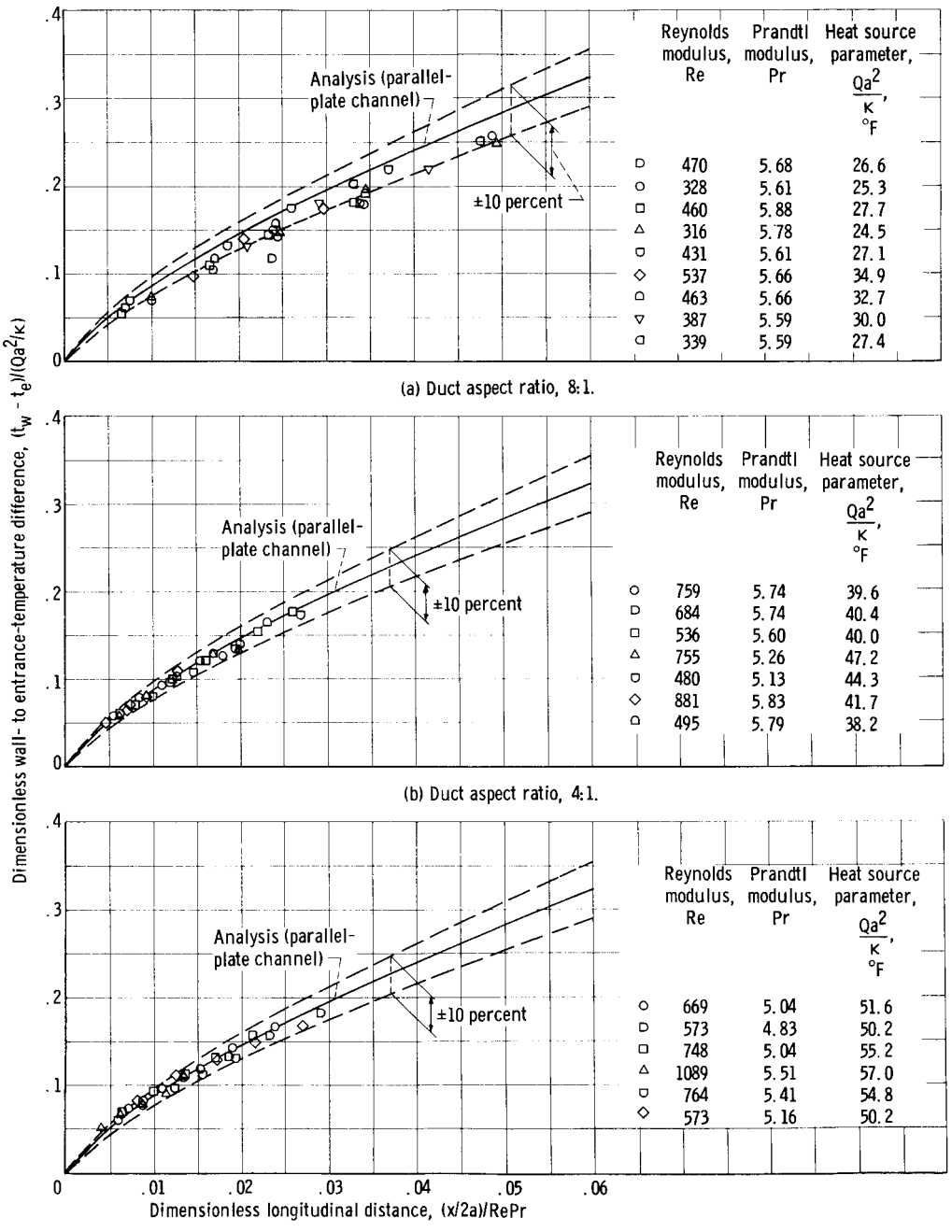

Figure 10. - Longitudinal variation of wall- to entrance-temperature difference measured in corner of channel.

difference in a corner (Y = Z = 1) of the 8:1 duct and is compared with a curve calculated from the theoretical relation equation (4) for the parallel-plate channel. The experimental results lie slightly lower than the theoretical result and, as with the centerline data cited previously, exhibit some scatter (about 10 percent). Results of the measurements for the 4:1 and 1:1 ducts and comparison with the theoretical results for the parallel-plate channel are shown in figures 10(b) and (c), respectively. It is observed that the measured dimensionless temperature differences are in good agreement with the theoretical (deviation <10 percent) and in addition, although perhaps not immediately apparent, lie somewhat below the corresponding centerline data. The fact that the dimensionless temperature difference $(t_w - t_e)/(Qa^2/\kappa)$ is less in the corner than at the centerline for each aspect ratio duct is somewhat surprising. This effect is possibly due to some conduction of heat into the top and side walls, and to the reduction in ion mobility in the corner (refs. 20 and 21), which would produce a somewhat transversely nonuniform internal heat generation. As will be described on page 23, additional measurements were made of the transverse wall temperature distributions at specific longitudinal positions to further investigate this result.

Perhaps another quantity of practical interest is the variation of the wall- to bulk-temperature difference as a function of position along the duct. The increase of the bulk temperature per unit length, dt_b/dx, was obtained under the assumption that the bulk temperature varies linearly between the measured temperatures at the entrance and exit cross sections. The theoretical relation equation (4) indicates that this assumption is correct for a parallel-plate channel with uniform internal heat sources.

Dimensionless wall- to bulk-temperature variations using the wall temperature measured at the centerline of the upper wall (Y = 1, Z = 0) and using the temperature measured in the corner (Y = Z = 1) are presented in figures 11 and 12 (pgs. 20 and 21), respectively, for the 8:1, 4:1, and 1:1 ducts and are compared with curves calculated from the theoretical relation equation (6) for a parallel-plate channel. It is observed from figure 11 that the data in general exhibit some scatter, which diminishes as the aspect ratio decreases. The experimental results for the ducts with rectangular cross section lie somewhat above the theoretical curve and the results for the square duct. On the whole, the agreement between the measured and theoretical temperature differences may be termed satisfactory when the experimental uncertainties are considered, particularly the possibility of a slightly transversely variable internal heat generation.

Figure 12 shows the dimensionless wall- to bulk-temperature variation in the corner of each of the three aspect ratio ducts. The experimental results for the ducts with rectangular cross section lie somewhat below the theoretical curve and the results for the square duct. No explanation for the scatter exhibited by the data for the 8:1 duct is known. About the same level of agreement between the measured and theoretical temperature differences is exhibited in the corner region as along the centerline of the top wall

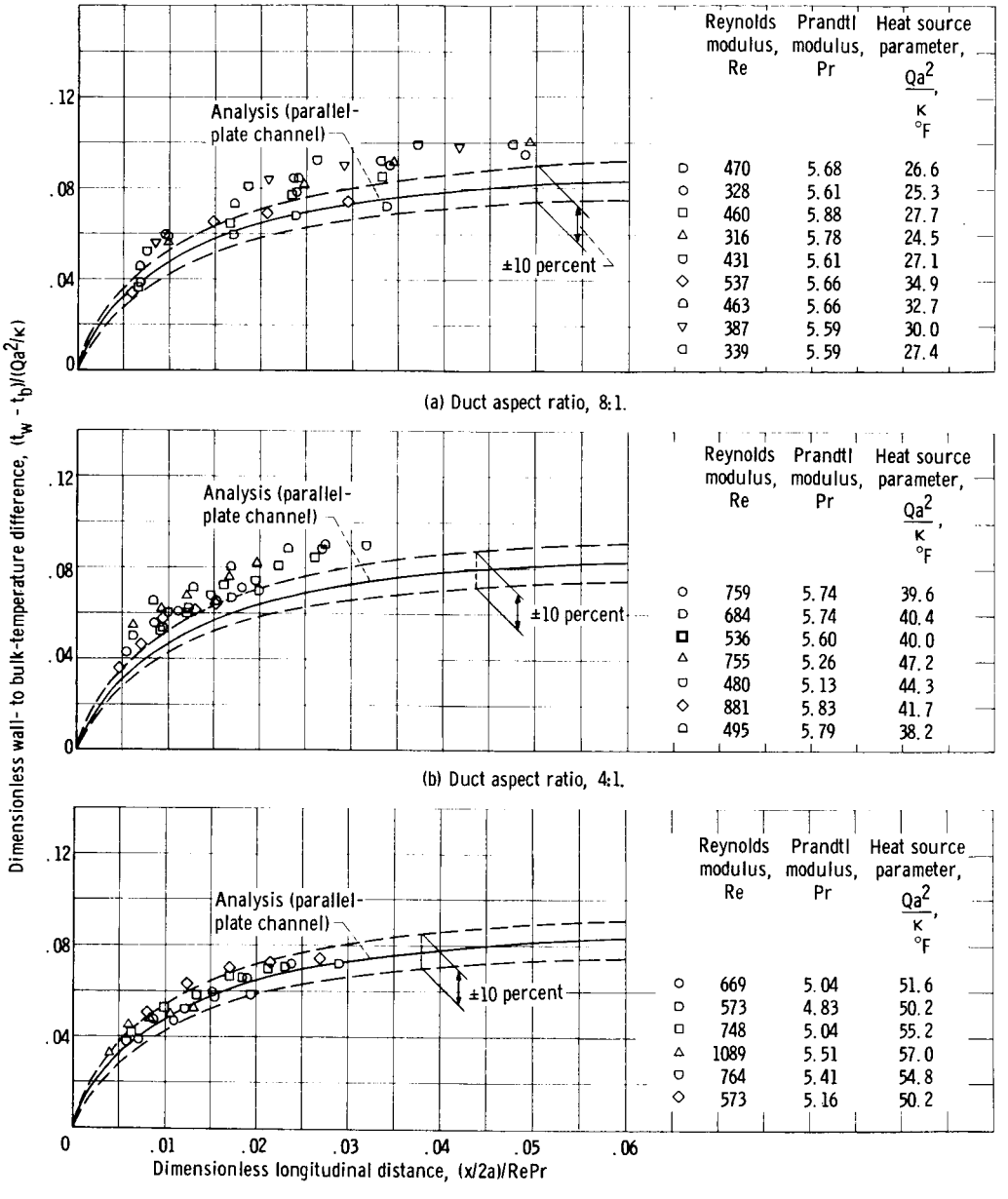

Figure 11. - Longitudinal variation of local wall- to bulk-temperature difference measured at centerline of top wall.

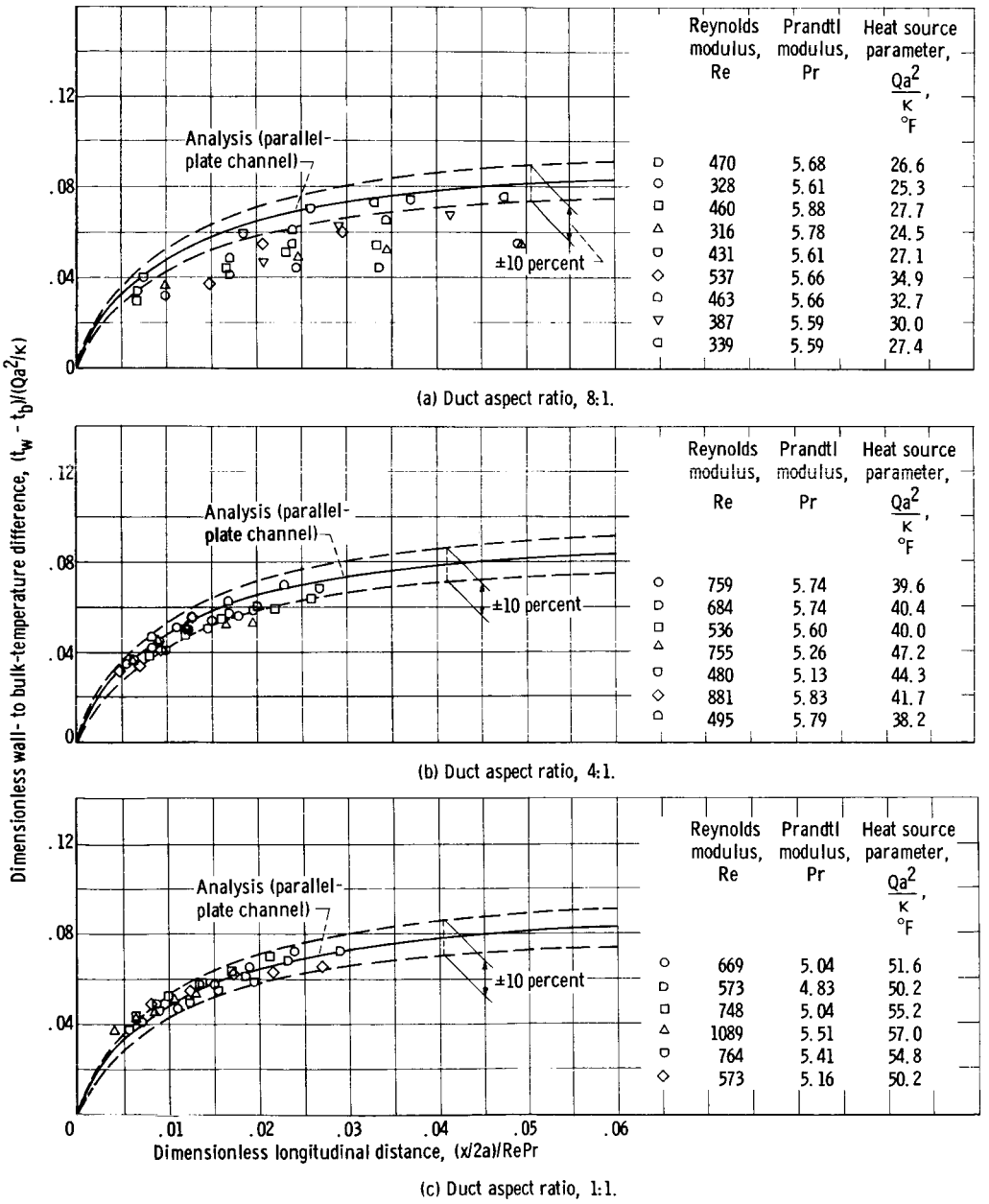

(a) Duct aspect ratio, 8:1.

Reynolds modulus, Re	Prandtl modulus, Pr	Heat source parameter, $\frac{Qa^2}{K}$, °F
470	5.68	26.6
328	5.61	25.3
460	5.88	27.7
316	5.78	24.5
431	5.61	27.1
537	5.66	34.9
463	5.66	32.7
387	5.59	30.0
339	5.59	27.4

(b) Duct aspect ratio, 4:1.

Reynolds modulus, Re	Prandtl modulus, Pr	Heat source parameter, $\frac{Qa^2}{K}$, °F
759	5.74	39.6
684	5.74	40.4
536	5.60	40.0
755	5.26	47.2
480	5.13	44.3
881	5.83	41.7
495	5.79	38.2

(c) Duct aspect ratio, 1:1.

Reynolds modulus, Re	Prandtl modulus, Pr	Heat source parameter, $\frac{Qa^2}{K}$, °F
669	5.04	51.6
573	4.83	50.2
748	5.04	55.2
1089	5.51	57.0
764	5.41	54.8
573	5.16	50.2

Figure 12. - Longitudinal variation of local wall- to bulk-temperature difference measured in corner of channel.

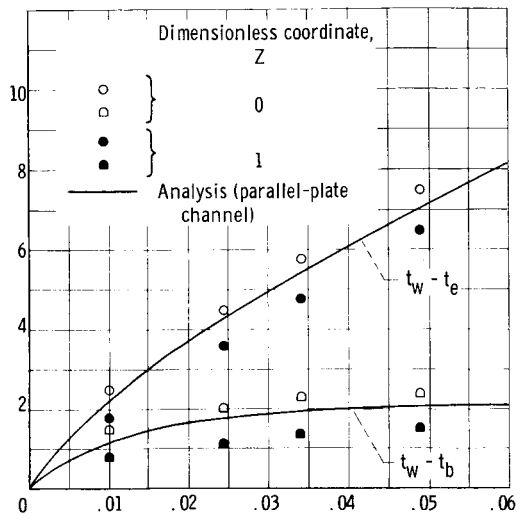

(a) Duct aspect ratio, 8:1. Reynolds number, 328; heat generation rate per volume, 5160 Btu per hour per cubic foot.

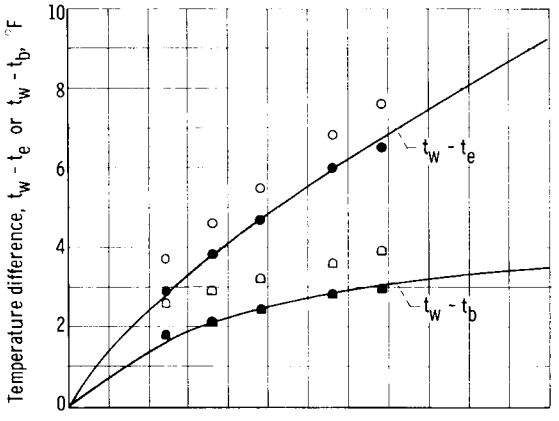

(b) Duct aspect ratio, 4:1. Reynolds number, 755; heat generation rate per volume, 9725 Btu per hour per cubic foot.

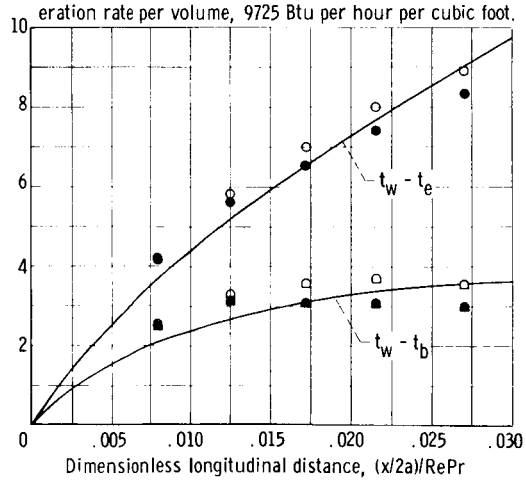

(c) Duct aspect ratio, 1:1. Reynolds number, 573; heat generation rate per volume, 10 450 Btu per hour per cubic foot.

Figure 13. - Representative longitudinal distribution of wall- to entrance- or wall- to bulk-temperature difference.

(fig. 11) for all aspect ratios of this investigation.

It is illuminating to present local results in detail to give a clearer picture of the wall-temperature development for the three aspect ratio ducts. For brevity local results will be given in detail only for a single representative run for each aspect ratio. The local results for other Reynolds numbers and heat generation rates do not differ significantly from those presented, aside from some experimental scatter.

Representative longitudinal and transverse temperature profiles for the 8:1, 4:1, and 1:1 aspect ratio ducts are shown in figures 13(a), (b), and (c), respectively. The ordinate of the figures is the difference between the local wall temperature and the entering fluid temperature or else the difference between the local wall temperature and the local bulk temperature.

These measurements indicate reasonable agreement between the experimental points and the profile calculated from the theoretical result for a parallel-plate channel. As mentioned previously, the experimental results measured at the centerline of the top wall (Z = 0) fall above those measured in the corresponding corner for all aspect ratios and Reynolds numbers of this investigation. It would be expected that if the internal heat generation was transversely as well as longitudinally uniform, hot spots would occur in the corners caused by the poor convection due to the low velocities in the corners region. The fact that the temperature differences $t_w - t_e$ and $t_w - t_b$ decrease in the corners is believed due to the retardation of the speed of the ions in the corners. The ions in their

motion through the solvent are subjected to a viscous drag, due to the viscous properties of the solvent. The viscous drag is highest in the corner regions, where the flow velocities are least, and thus the speed of the ions is reduced in these regions. Since the electric conduction process depends on the mobility of the ions through the solution, the quantity of electrical current passed through the solution in the corners must be somewhat less than that along the centerline. This produces a slightly nonuniform distribution of current that undoubtedly gives rise to a slight variation in the heat-source distribution in the transverse z-direction. This slight nonuniformity is apparently sufficient to suppress the hot spots in the corners. It might be thought that conduction of heat into the duct walls forming the corner would also aid this effect. The lucite duct walls, however, have a thermal conductivity of 0.024 to 0.24 Btu per hour per foot per ^{o}F, and, in addition, are backed with fiber glass insulation. An adiabatic wall condition is therefore closely approximated, and calculations show that the heat loss through the walls for the present experimental conditions is negligible.

To further substantiate the assumption that the heat generation has a slight nonuniformity in the transverse z-direction, additional wall-temperature measurements were made through the addition of more thermocouples along the top wall at the specified longitudinal positions. The thermocouples were added at the locations $Z = -1.00$, 0.50, and 0.75 for the 8:1 duct, and at $Z = -1.00$, -0.50, and 0.50 for the 4:1 duct. The relatively narrow width of the square duct made such additional measurements impractical.

It would be expected that if the ion speed in the electrolytic solution is reduced, and hence the electric current flow, as the corner region is approached, the transverse temperatures at a given axial location would decrease from the centerline value, and thus hot spots would exist at the centerline location ($Y = 1$, $Z = 0$). Representative longitudinal and transverse temperature profiles for the 8:1 and 4:1 aspect ratio ducts are shown in figures 14(a) and (b) (p. 24), respectively. The local results for other Reynolds numbers and other heat generation rates do not differ greatly from those presented. It can be seen from the figures that the transverse temperatures at each axial position do not exceed the centerline temperature value and that the temperature decreases in the corners. The slight asymmetry of the temperature profiles is due to the scatter of the data. The analytical results obtained from the parallel-plate channel analysis predict a single value, at a given axial location, for $t_w - t_e$ and for $t_w - t_b$. An important practical consequence is that the parallel-plate model cannot be used to predict peripheral temperature variations in finite aspect ratio ducts.

It has become customary in applications involving flow and heat transfer in ducts with noncircular cross section to base the Reynolds and Graetz number for such cross sections on a length that is called the hydraulic diameter and is defined by the equation

$$d_H \equiv 4 \frac{\text{Flow cross-sectional area}}{\text{Wetted perimeter}}$$

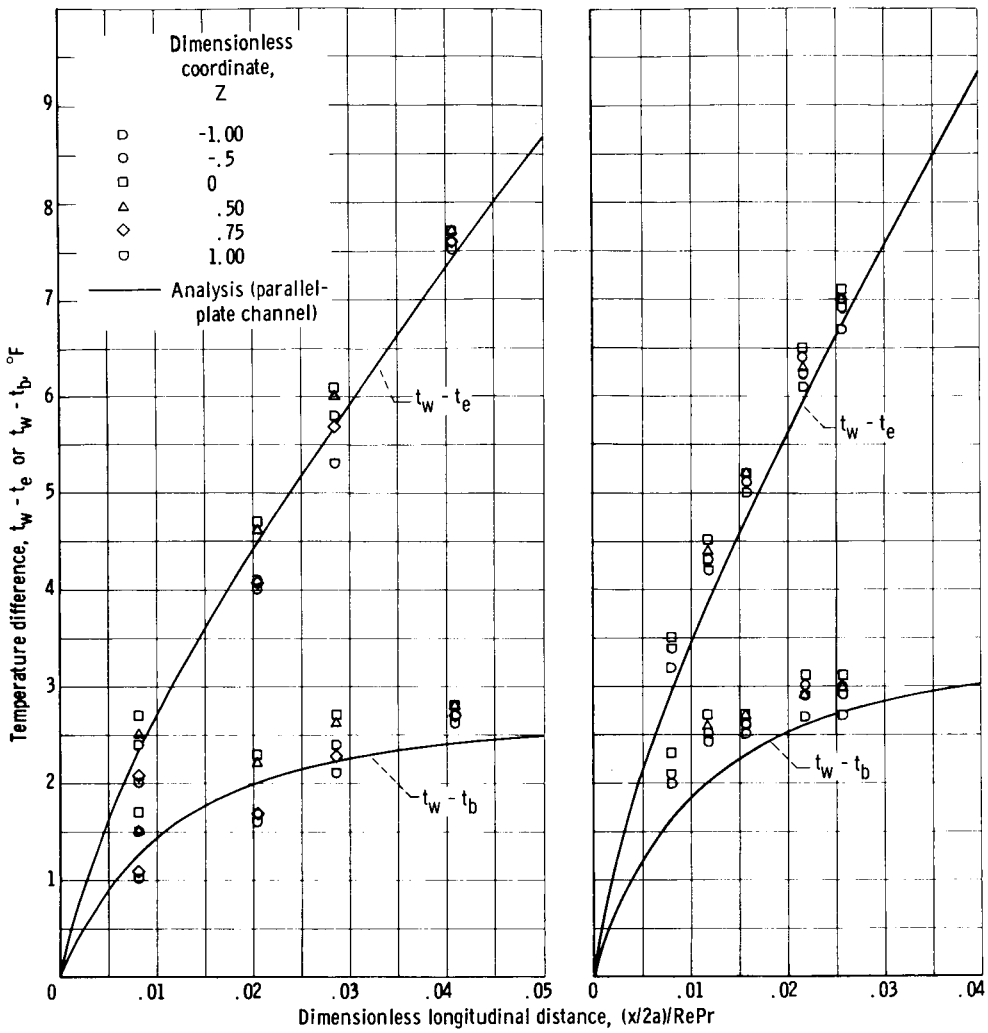

(a) Duct aspect ratio, 8:1. Reynolds number, 332; heat generation rate per volume, 6100 Btu per hour per cubic foot.

(b) Duct aspect ratio, 4:1. Reynolds number, 458; heat generation rate per volume, 7750 Btu per hour per cubic foot.

Figure 14. - Representative longitudinal and transverse temperature distributions measured at top wall of duct.

There are two basic reasons for this practice. First, a Graetz number built with the hydraulic diameter as the characteristic duct dimension may provide equally good, or perhaps better, single-line correlation of experimental data regardless, for example, of the duct aspect ratios.

The use of an effective diameter (e.g., the hydraulic diameter) as the characteristic dimension of a noncircular passage has also led to the result that fully developed heat-transfer data for a number of shapes agree quite closely with data for a circular tube of diameter equal to the effective diameter of the noncircular passage. This method of approach has been found to be sufficiently accurate for heat-transfer situations in which either the wall temperature or wall heat flux is prescribed.

It seems natural, therefore, to examine the use of the hydraulic diameter in attempt-

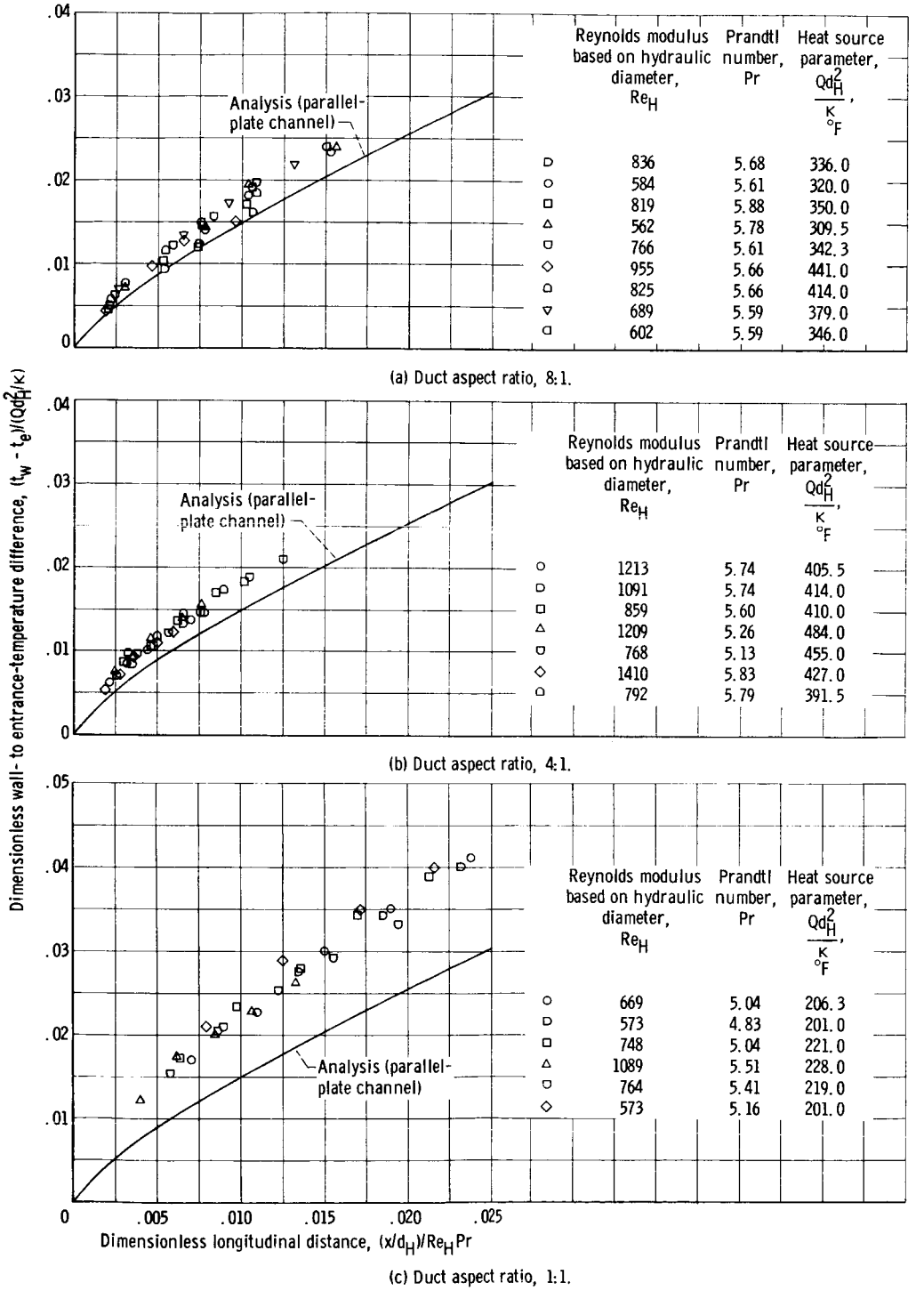

Figure 15. - Longitudinal variation of wall- to entrance-temperature difference measured at centerline of top wall. Heat source parameter and reciprocal Graetz number based on hydraulic diameter.

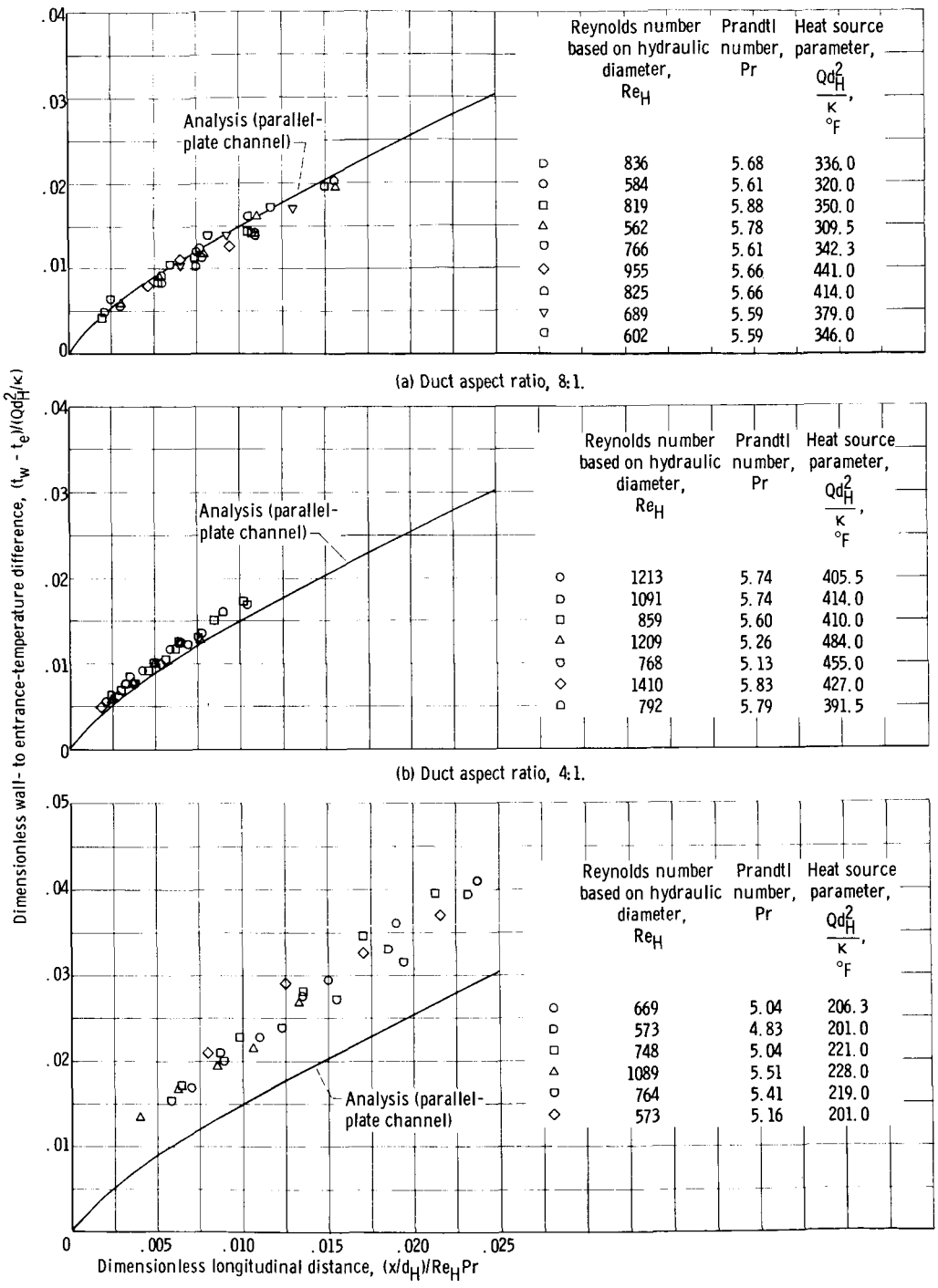

Figure 16. - Longitudinal variation of wall- to entrance-temperature difference measured in corner of channel. Heat source parameter and reciprocal Graetz number based on hydraulic diameter.

ing to correlate the present experimental heat-transfer data in the thermal entrance region with the parallel-plate channel analysis. In addition, the hydraulic diameter concept is examined in an attempt to correlate the experimental data and parallel-plate channel analysis with the circular tube analysis. Hence, the hydraulic diameter for a rectangular duct, given by

$$d_H = \frac{4a}{1 + (1/\gamma)}$$

is used as the characteristic dimension, rather than the duct dimension a, in the appropriate equations and data.

Figures 15 and 16 show the dimensionless wall- to entrance-temperature difference $(t_w - t_e)/(Qd_H^2/\kappa)$ at the centerline of the top wall and in a corner of the duct, respectively, plotted as a function of the modified reciprocal Graetz number $x/d_H Re_H Pr$ for the 8:1, 4:1, and 1:1 ducts. It is observed that fairly good correlation between the data for the rectangular cross sections and the analysis for a parallel-plate channel is achieved through the use of the hydraulic diameter. The experimental results for the square duct lie somewhat higher than the results for the ducts of rectangular cross section and are not correlated by the parallel-plate channel analysis.

The centerline experimental results for the three aspect ratio ducts are shown in figures 17 and 18 and are compared with the analytical results for the circular tube and for the parallel-plate channel. Both analytical studies were carried out for the case of uniform internal heat generation. The characteristic dimension used in both the dimensionless temperature differences and dimensionless longitudinal distance (or modified reciprocal Graetz number) is the hydraulic diameter d_H. For a tube of circular cross section, d_H reduces simply to the tube diameter. It is seen from figure 17 that the analysis for the parallel-plate channel is not correlated by the circular tube analysis. The parallel-plate channel analysis yields results for

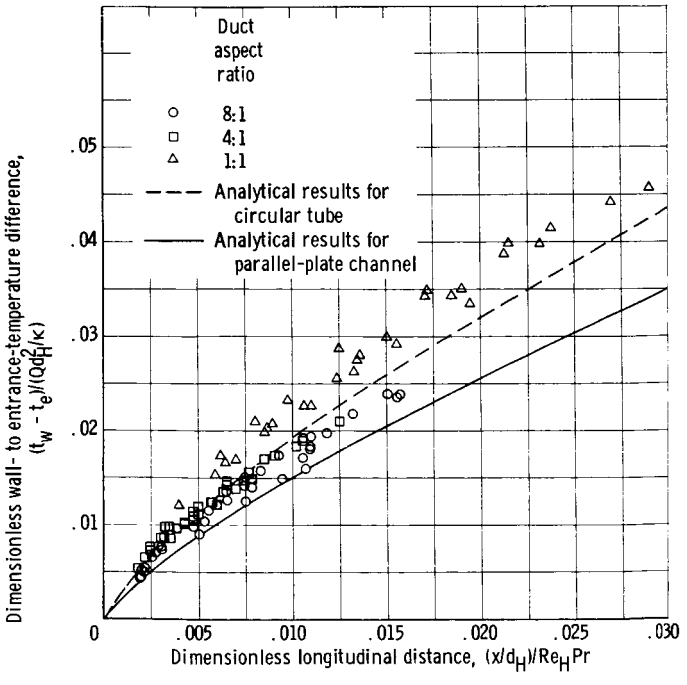

Figure 17. - Comparison of analytical and experimental results for longitudinal variation of dimensionless wall- to entrance-temperature difference with hydraulic diameter used as geometry dimension.

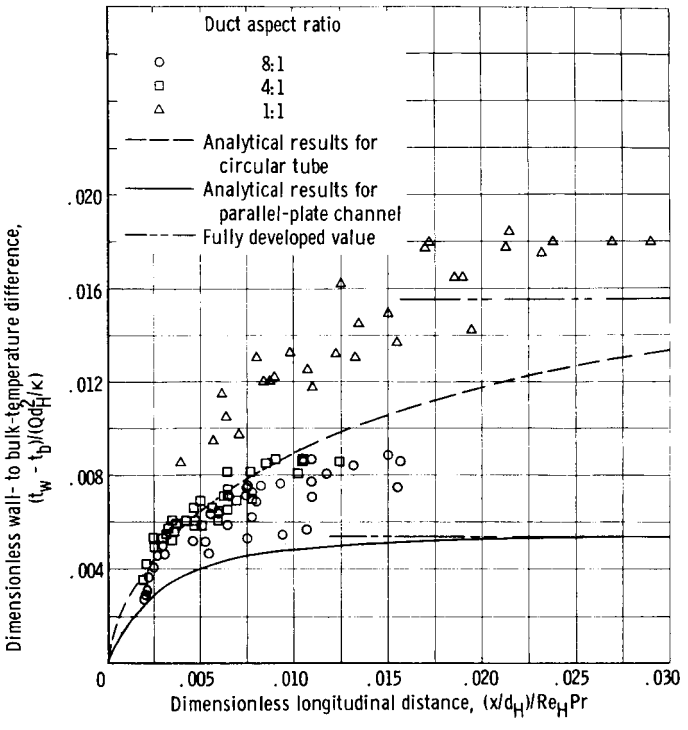

Figure 18. - Comparison of analytical and experimental results for longitudinal variation of dimensionless local wall- to bulk-temperature difference with hydraulic diameter used as geometry dimension.

$(t_w - t_e)/(Qd_H^2/\kappa)$ which are lower than those for the circular tube. The experimentally determined values of $(t_w - t_e)/(Qd_H^2/\kappa)$ for the ducts with rectangular cross section are, apart from some scatter, bracketed by the results of the two analyses. The experimental results for the square duct lie slightly higher than the analysis for either the parallel-plate channel or the circular tube.

The dimensionless local wall- to bulk-temperature differences for the three aspect ratio ducts are shown in figure 18 as a function of the dimensionless longitudinal distance. Again it can be seen that the results of the parallel-plate channel analysis are different than those for the circular tube. The experimentally determined values for the 8:1 and 4:1 ducts are bracketed by the results of the two analyses, apart from some scatter, while the experimental results for the square duct are significantly higher than the predicted values for either flow passage.

It is perhaps of interest at this point to determine if the hydraulic diameter is a meaningful parameter in determining the thermal entrance length for the rectangular ducts.

The fully developed dimensionless values of wall- to bulk-temperature difference for a circular tube and for a parallel-plate channel, respectively, are given by

$$\frac{t_w - t_b}{Qr_0^2/\kappa} = \frac{1}{16} \qquad \text{(circular tube)} \tag{11a}$$

$$\frac{t_w - t_b}{Qa^2/\kappa} = \frac{3}{35} \qquad \text{(parallel-plate channel)} \tag{11b}$$

When these results are converted to dimensionless temperature differences based on the use of the hydraulic diameter, there is obtained

$$\frac{t_w - t_b}{Qd_H^2/\kappa} = \frac{1}{64} = 0.0156 \qquad \text{(circular tube)} \tag{12a}$$

$$\frac{t_w - t_b}{Qd_H^2/\kappa} = \frac{3}{560} = 0.0054 \qquad \text{(parallel-plate channel)} \tag{12b}$$

These asymptotic values are shown in figure 18. The results indicate that the wall- to bulk-temperature profiles become fully developed at widely different values of the reciprocal Graetz number (based on the hydraulic diameter), or in other words, at different distances from the entrance to the heating section.

From equation (11b), there is obtained for the parallel-plate channel

$$\frac{t_w - t_b}{Qa^2/\kappa} = \frac{3}{35} = 0.0857$$

as the fully developed value. It is practice to define a thermal entrance length as the length required to develop the wall- to bulk-temperature difference to within 5 percent of the fully developed value. Hence the reciprocal Graetz number (based on the duct dimension a) required to attain the thermal entrance length L_e is found from figures 11 and 12 to be

$$\frac{L_e/2a}{RePr} = 0.05$$

Inasmuch as the experimental data shown in these figures are in reasonable agreement with the parallel-plate channel analysis for the three aspect ratios investigated, it is concluded that the reciprocal Graetz number required for developing the temperature profiles within 5 percent of the fully developed value is a constant, when based on the duct dimension a, and is essentially independent of aspect ratio.

These results indicate that the hydraulic diameter concept is not applicable for laminar heat transfer in rectangular ducts with internal heat sources in the fluid stream. As a result of the rather good agreement between the theoretical calculations for the parallel-plate channel and the experimental data for the aspect ratio ducts with the use of the distance between upper and lower plates as the characteristic dimension, the equations (4), (5), and (6) are recommended for the practical calculation of heat transfer in rectangular passages in the presence of internal heat generation in the fluid stream.

Effect of Free Convection

As mentioned previously, an additional complication in the determination of heat-transfer characteristics of duct flow that can arise is caused by the fact that frequently, for the low velocities necessary for laminar flow, eddy currents by free convection change the flow pattern, and hence a combination of forced and free convection possibly results. In a fluid in which the density varies with the temperature (such as with the fluid used for the present investigation) bouyancy forces present in a forced-convection flow produce free-convection effects, and it is of interest to know when they can be neglected and when they have to be taken into account.

It has to be expected that Reynolds, Prandtl, and Grashof numbers are among the more important influencing parameters. For very large Reynolds values and very small Grashof numbers, the influence of free convection on the heat transfer should be negligible. For very large Grashof values and very small Reynolds numbers, however, the free convection should be the dominating factor for a given value of the Prandtl number.

For laminar horizontal flow in rectangular ducts with internal heat generation in the fluid stream, it appears that analytical studies of natural convection effects have thus far been extended only to the fully developed flow between parallel plates with a linear axial temperature distribution and with uniform internal heat generation (ref. 24). The linear axial temperature distribution implies thermally fully developed flow, achieved far down the channel. Inasmuch as no analyses have been made of natural convection effects in the thermal entrance region, the analytical results presented in reference 24 were used to analyze the experimental data of the present investigation for natural convection effects with the expectation that the actual situation is satisfactorily approximated.

The fully developed velocity distribution within the channel with combined free and forced convection is given in reference 24 as

$$\frac{u}{\bar{u}} = 6(\omega - \omega^2) + \frac{N_1}{24}(4\omega^3 - 6\omega^2 + 2\omega) \tag{13}$$

where

$$\omega = \frac{\xi}{2a} \tag{14}$$

$$N_1 = \frac{Gr}{Re} \tag{15}$$

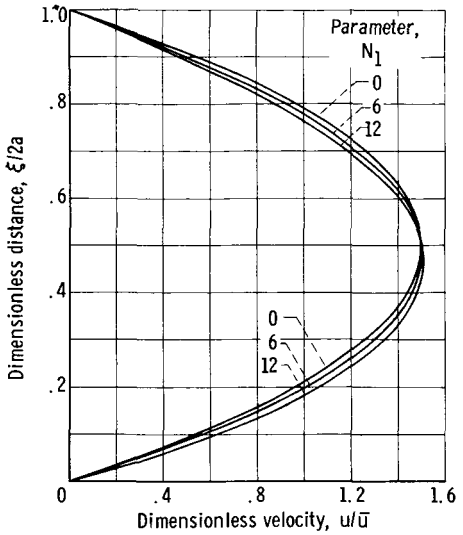

Figure 19. - Fully developed velocity distribution in parallel-plate channel with combined forced and free convection.

$$Gr = \frac{16\beta g a^4}{\nu^2} \frac{dt}{dx} \tag{16}$$

The bottom plate corresponds to $\omega = 0$. Equation (13) shows that the velocity field depends on the ratio of the Grashof modulus to the Reynolds modulus. The first term of equation (13) is the plane Poiseuille distribution and is therefore the forced convection contribution. Figure 19 presents a plot of the velocity profile for values of the parameter N_1 of 0, 6, and 12. It can be seen that even for a value of $N_1 = 12$ the velocity profile is only slightly altered from the plane Poiseuille result (obtained for $N_1 = 0$). On the basis of this figure, it was decided arbitrarily to select a value of N_1 approximately equal to 6 as the upper limit for the ratio of Grashof-to-Reynolds moduli of the experimental data. When the value of N_1 exceeded approximately 6.6 for a run, the results were not considered. The bulk temperature gradient was selected as the linear axial temperature gradient in evaluating the experimental Grashof modulus.

The influence of radial viscosity variations, viscous dissipation, unequal wall heat fluxes, and uniform internal heat generation on the fully developed temperature field has been considered in reference 24. If all but the last influence are considered negligible or not applicable, it can be shown that the temperature distribution within the channel with combined free and forced convection is given by the result

$$\frac{t - t_{w,0}}{Qa^2/\kappa} = 4\omega^3 - 2\omega^4 - 2\omega^2 + \frac{N_1}{180}(6\omega^5 - 15\omega^4 + 10\omega^3) \tag{17}$$

where $t_{w,0}$ is the lower wall temperature at $\omega = 0$. To find the difference between the upper wall temperature $t_{w,1}$ and the lower wall temperature in the presence of combined forced and free convection, it is only necessary to set $\omega = 1$ in equation (17); this yields

$$\frac{t_{w,1} - t_{w,0}}{Qa^2/\kappa} = \frac{N_1}{180} \tag{18}$$

Figure 20 (p. 32) presents a plot of the temperature profile given by equation (17) for values of the parameter N_1 of 0, 6, and 12. It is seen that an increase in the value of

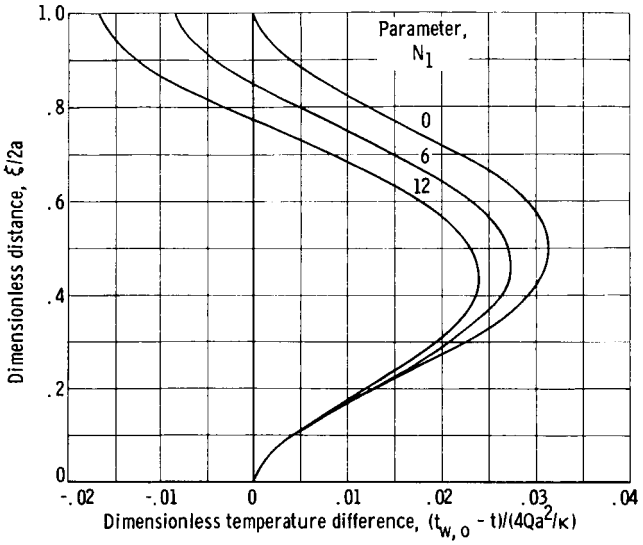

Figure 20. - Fully developed temperature distribution in a parallel-plate channel with combined forced and free convection.

N_1 increases the upper wall temperature above the value of the lower wall temperature, which causes an increased tendency toward flow instability in the channel. In addition, for a given value of N_1, increased values of Qa^2/κ increase the wall-temperature difference $t_{w,1} - t_{w,0}$. It is clear from equation (18) that $t_{w,1} > t_{w,0}$ for $N_1 > 0$. An estimate of the maximum effect of free convection on the wall-temperature difference $t_{w,1} - t_{w,0}$ for the present experimental investigations can be made by using equation (18) and employing the maximum experimental values of N_1 and Qa^2/κ occurring for a given run. These were found to be 6.6° and 50.2° F, respectively, and were obtained in the course of the investigation of the square duct. Inserting these values into equation (18) yields the result $(t_{w,1} - t_{w,0})_{max} = 1.9^\circ$ F. In almost all of the remaining experimental runs for the aspect ratio ducts the values of N_1 and Qa^2/κ led to the theoretical value of the wall-temperature difference being considerably less than this value. The smallest value for $t_{w,1} - t_{w,0}$ was, for example, 0.25° F and occurred for the experimental values of $N_1 = 1.61$ and $Qa^2/\kappa = 27.7^\circ$ F obtained for the 8:1 duct. It is worth noting that the greatest uncertainty regarding free-convection effects on the experimental data occurs for the data for the 1:1 aspect ratio duct owing to the fact that for a given value of N_1 the parameter Qa^2/κ is largest for this duct.

There are neither experimental measurements nor analytical solutions of the natural convection effects in the thermal entrance length in forced horizontal flows in rectangular passages. Therefore, support for the assumption that the effect of free convection on the present experimentally determined velocity and temperature pattern can be neglected can only come, by inference, from the foregoing comparisons and estimates. In view of the results, however, it is felt that the assumption of a negligibly small contribution of free convection to the experimental findings of the present investigation is at least partially substantiated; hence, the experimental data presented may be deemed reasonably reliable.

CONCLUSIONS

An experimental investigation was conducted of laminar forced-convection flow of a heat-generating fluid in passages with rectangular cross sections. Wall-temperature measurements were made for fully developed flow in ducts with aspect ratios of 1:1, 4:1, and 8:1, with an approximately uniform heat generation in the fluid stream. The data obtained from the three rectangular ducts have been compared with the analytical results for a parallel-plate channel and for a circular tube, both analytical studies being carried out for the case of uniform internal heat generation.

The comparisons with the analytical results indicate the following conclusions:

1. The longitudinal variation of wall temperature in finite aspect ratio ducts can be predicted with engineering accuracy (10-percent deviation) from the analytical results for the parallel-plate channel when the half length of the short side of the rectangular duct is used as the characteristic dimension.

2. The longitudinal variation of the difference between the local wall temperature and fluid bulk temperature can be satisfactorily predicted for a rectangular duct from the parallel-plate channel analysis when the half-length of the short side of the duct is used as the characteristic dimension.

3. Correlation of the experimental heat-transfer data along a single line is not achieved through the use of the hydraulic diameter as the representative duct dimension.

4. The hydraulic diameter concept, which implies that heat-transfer data for laminar flow in a noncircular passage can be correlated with relations, or experimental data, for a circular tube by use of the hydraulic diameter, is not applicable for laminar heat transfer in rectangular ducts with internal heat generation in the fluid stream.

5. For the three aspect-ratio ducts investigated, the reciprocal Graetz number (based on the length of the short side of the duct) required to attain the thermal entrance length is a constant and is essentially independent of aspect ratio.

Lewis Research Center,
National Aeronautics and Space Administration,
Cleveland, Ohio, July 6, 1965.

APPENDIX - SYMBOLS

A_c cross-sectional area of duct

A_n coefficients in series expansion

a half-length of short side of rectangular duct

b half-length of long side of rectangular duct

c_p specific heat at constant pressure

d_H hydraulic diameter, $4 A_c$/wetted perimeter

Gr Grashof modulus, $(16\beta g a^4/\nu^2)(dt/dx)$

g gravitational acceleration

L length of test section

L_e length of thermal entrance region

N_1 ratio of Grashof modulus to Reynolds number, Gr/Re

Pr Prandtl modulus, $\mu c_p/\kappa$

Q rate of internal heat generation per unit volume

q_e electrical heat input

Re Reynolds modulus, $2\rho\bar{u}a/\mu$

Re_H Reynolds modulus based on hydraulic diameter, $\rho\bar{u}d_H/\mu$

r_0 radius of circular tube

t temperature

u fluid velocity

w weight flow rate, $\rho\bar{u}A_c$

x axial coordinate along duct length

Y dimensionless coordinate, y/a

Y_n eigenfunctions of eq. (3)

y coordinate along short side of rectangular duct

Z dimensionless coordinate, z/b

z coordinate along long side of rectangular duct

β coefficient of thermal expansion

γ aspect ratio of rectangular duct, b/a

κ thermal conductivity of fluid

λ_n eigenvalues of eq. (3)

μ fluid viscosity

ν fluid kinematic viscosity

ξ transposed coordinate along short side of rectangular passage, y + a

ρ fluid density

ω dimensionless coordinate, $\xi/2a$

Subscripts:

b fluid bulk condition

e value at duct entrance x = 0

w value at broad wall

0 lower broad wall, y = -a

1 upper broad wall, y = a

Superscript:

$(\bar{\ })$ average value

REFERENCES

1. Topper, L.: Forced Heat Convection in Cylindrical Channels. Chem. Eng. Sci., vol. 5, 1956, pp. 13-19.

2. Sparrow, E. M.; and Siegel, Robert: Laminar Tube Flow with Arbitrary Internal Heat Sources and Wall Heat Transfer. Nucl. Sci. Eng., vol. 4, no. 2, Aug. 1958, pp. 239-254.

3. Siegel, Robert; and Sparrow, E. M.: Turbulent Flow in a Circular Tube with Arbitrary Internal Heat Sources and Wall Heat Transfer. J. Heat Transfer (Trans. ASME), ser. C, vol. 81, no. 4, 1959, pp. 280-290.

4. Schechter, R. S.; and Wissler, E. H.: Heat Transfer to Bingham Plastics in Laminar Flow Through Circular Tubes with Internal Heat Generation. Nucl. Sci. Eng., vol. 6, no. 5, Nov. 1959, pp. 371-375.

5. Foraboschi, Franco P.; and Di Federico, Iginio: Heat Transfer in Laminar Flow of Non-Newtonian Heat-Generating Fluids. Int. J. Heat and Mass Transfer, vol. 7, no. 3, Mar. 1964, pp. 315-325.

6. Poppendiek, H. F.: Forced-Convection Heat Transfer in Pipes with Volume Sources Within the Fluids. Nucl. Eng., Part I: Chem. Eng. Prog. Symposium Ser., vol. 50, no. 11, 1954, pp. 93-104.

7. Petukhov, B. S.; and Genin, L. G.: Heat Transfer in Tubes with Internal Heat Sources in the Fluid Stream. Int. Chem. Eng., vol. 3, no. 4, Oct. 1963, pp. 483-486.

8. Inman, Robert M.: Experimental Study of Temperature Distribution in Laminar Tube Flow of a Fluid with Internal Heat Generation. Int. J. Heat and Mass Transfer, vol. 5, no. 11, Nov. 1962, pp. 1053-1058.

9. Tao, L. N.: On Some Laminar Forced-Convection Problems. J. Heat Transfer (Trans. ASME), ser. C, vol. 83, no. 4, Nov. 1961, pp. 466-472.

10. Tao, L. N.: The Second Fundamental Problem in Heat Transfer of Laminar Forced Convection. J. Appl. Mech. (Trans. ASME), ser. E, vol. 29, no. 2, June 1962, pp. 415-420.

11. Tao, L. N.: Method of Conformal Mapping in Forced Convection Problems. Int. Developments in Heat Transfer, pt. III, sec. A, (ASME), 1961, pp. 598-606.

12. Perlmutter, Morris; and Siegel, Robert: Heat Transfer to an Electrically Conducting Fluid Flowing in a Channel with a Transverse Magnetic Field. NASA TN D-875, 1961.

13. Michiyoshi, Itaru; and Matsumoto, Ryuichi: Heat Transfer by Hartmann's Flow in Thermal Entrance Region. Int. J. Heat and Mass Transfer, vol. 7, no. 1, Jan. 1964, pp. 101-112.

14. Sparrow, E. M.; Novotny, J. L.; and Lin, S. H.: Laminar Flow of a Heat-Generating Fluid in a Parallel-Plate Channel. A.I.Ch.E. J., vol. 9, no. 6, Nov. 1963, pp. 797-804.

15. Sparrow, E. M.; and Siegel, R.: Applications of Variational Methods to the Thermal Entrance Region of Ducts. Int. J. Heat and Mass Transfer, vol. 1, nos. 2/3, Aug. 1960, pp. 161-172.

16. Han, L. S.: Hydrodynamic Entrance Lengths for Incompressible Laminar Flow in Rectangular Ducts. J. Appl. Mech. (Trans. ASME), ser. E, vol. 27, no. 3, Sept. 1960, pp. 403-409.

17. Timoshenko, S.; and Goodier, J. N.: Theory of Elasticity. Second ed., McGraw-Hill Book Co., Inc., 1951.

18. Sparrow, E. M.; and Siegel, R.: A Variational Method for Fully Developed Laminar Heat Transfer in Ducts. J. Heat Transfer (Trans. ASME), ser. C, vol. 81, no. 2, May 1959, pp. 157-167.

19. Ramo, Simon; and Whinnery, John R.: Fields and Waves in Modern Radio. Second ed., John Wiley & Sons, Inc., 1953.

20. Newman, F. H.: Electrolytic Conduction. Chapman and Hall, Ltd., London, 1930.

21. Glasstone, S.: The Electrochemistry of Solutions. Second ed., D. Van Nostrand Co., Inc., 1937.

22. Hodgman, C. D., ed.: Handbook of Chemistry and Physics. Thirty-second ed., Chem. Rubber Pub. Co., 1950.

23. Lange, N. A., ed.: Handbook of Chemistry. Eighth ed., Handbook Pub. Inc., 1952.

24. Gill, William N.; and Del Casal, Eduardo: A Theoretical Investigation of Natural Convection Effects in Forced Horizontal Flows. A.I.Ch.E. J., vol. 8, no. 4, Sept. 1962, pp. 513-518.